Low Temperature Induced Highly Stable Zn Metal Anodes for Aqueous Zinc-ion Batteries

Huibing He [a, *], Hongyu Qin [a], Fang Shen [a], Nan Hu [a], Jian Liu [b, *]

[a] *School of Chemistry and Chemical Engineering, Guangxi Key Laboratory of Electrochemical Energy Materials, Guangxi University, Nanning 530004, PR China*

[b] *School of Engineering, Faculty of Applied Science, The University of British Columbia, Kelowna, BC V1V 1V7 Canada*

Experimental Section

1. *Zn foil pretreatment*

Zinc foil (0.2 mm in thickness) was cut into round plates (Φ =14 mm) and cleaned by sonication sequentially in deionized water and absolute alcohol for 15 minutes, followed by nature drying before using as Zn metal anodes for ZIBs.

2. *Structural characterizations*

The crystal structure of the Zn foils before and after cycling was examined by Powder X-ray diffraction (XRD, Bruker D8-Advance X-ray diffractometer) using Cu Kα radiation (1.54056 Å). The morphology was observed by using a scanning electron microscope (SEM, Tescan MIRA3 FEGESEM) equipped with an energy-dispersive X-ray spectrometer (EDX). The Zn anodes were thoroughly washed with deionized water to remove residual salt and glass fiber before SEM observations. The optical images were obtained on a DMM-900C (Shanghai Caikon Optical Instrument Co., Ltd) metallographic microscope by using an *in-situ* optical electrochemical cell (Hefei in-situ Technology Co., Ltd). The contact angle between Zn and the electrolyte was measured by using a contact angle goniometer (Ramé Hart 260) with an electrolyte droplet of 5 μL.

3. *Electrochemical measurements*

CR2032 coin cells were assembled in air to evaluate electrochemical performance by testing on a Neware BTS 4000 battery tester. Zn|Zn symmetric cells were assembled with the same two zinc plates, glass fibers (separator, $\Phi = 5/8$ inch) and 3 M $Zn(SO_3CF_3)_2$ aqueous electrolyte. The electrolyte loading of Zn|Zn symmetric cells was set to be 120 μL. Electrochemical Impedance Spectroscopy (EIS) and linear polarization (corrosion test) were performed on a Biologic VSP Potentiostat/Galvanostat Station. EIS was conducted in a frequency range of 100 kHz to 0.01 Hz with a voltage amplitude of 5 mV. For the corrosion test, the working (WE), counter (CE), and reference (REF) electrodes were zinc, platinum, and Ag/AgCl, respectively. The linear polarization technique was applied to the system by scanning between −0.7 and 0.4 V *vs.* Ag/AgCl/KCl (3.5 M) from its open-circuit voltage (OCV) at a rate of 2 mV s^{-1} in 3 M $Zn(SO_3CF_3)_2$ solution. The hydrogen evolution performance was collected through LSV with a potential range of -0.9~-1.6 V (*vs.* Ag/AgCl) at a scan rate of 1 mV s^{-1}. The surface area of the working electrode was 1 (1 × 1) cm^2.

Table S1. Comparison of the electrochemical performance of Zn anodes in this work and others.

Symmetric cell configuration	**Current density (mA cm^{-2})**	**Lifespan (h)**	**Cumulative Specific Capacity (mAh cm^{-2})**	**Overpotential (mV)**	**Columbic efficiency (%)**	**Ref.**
Sc_2O_3@Zn	1	200	200	48	99.85 (1.13 mA cm^{-2}, 0.56 mAh cm^{-2})	[1]
3D ZnF_2@Zn	1	800	800	71.5	99.5 (5 mA cm^{-2}, 1 mAh cm^{-2})	[2]
ZnS@Zn	2	1100	2200	65	99.2 (2 mA cm^{-2}, 1 mAh cm^{-2})	[3]
PAM/PVP@Zn	0.2	2220	440	180	98.8 (1 mA cm^{-2}, 0.17 mAh cm^{-2})	[4]
β-PVDF@Zn	0.25	2000	500	80	96.5 (0.36 mA cm^{-2}, 0.18 mAh cm^{-2})	[5]
PANZ@Zn	1	1145	1145	150	99.8 (1 mA cm^{-2}, 1 mAh cm^{-2})	[6]
CNT@Zn	0.15	400	60	80	/	[7]
HsGDY@Zn	0.5	2400	1200	60	/	[8]
rGO@Zn	1	1200	1200	40	/	[9]
Bare Zn (0 °C)	1	>2500	> 2500	120	98.3 (0.5 mA cm^{-2}, 0.5 mAh cm^{-2})	This work

Table S2. EIS parameters obtained by fitting the data with the equivalent circuit in Figure 2a and Figure S5-S7.

Temperature		**0**	**5th**	**10th**	**15th**
0 ℃	R_s (Ω)	1.4	1.7	4.2	2.0
	R_{SEI} (Ω)	1978.0	15.6	15.1	13.8
	R_{CT} (Ω)	2075.0	81.7	59.0	35.9
20 ℃	R_s (Ω)	1.2	1.5	1.6	1.5
	R_{SEI} (Ω)	389.9	1.8	0.6	0.6
	R_{CT} (Ω)	537.5	29.0	19.0	16.1
50 ℃	R_s (Ω)	1.5	2.0	2.0	2.3
	R_{SEI} (Ω)	18.4	0.2	0.2	0.8
	R_{CT} (Ω)	186.0	4.9	4.2	5.1

Table S3 Electrochemical corrosion parameters of Zn metal foils at 0, 20, and 50 ℃.

Samples	**E_{corr} (mV)**	**I_{corr} (μA cm^{-2})**	**β_a (mV dec^{-1})**	**β_c (mV dec^{-1})**
0 ℃	-877.2	2.69	148.9	149.6
20 ℃	-895.8	5.75	155.5	155.7
50 ℃	-909.3	19.05	169.8	160.6

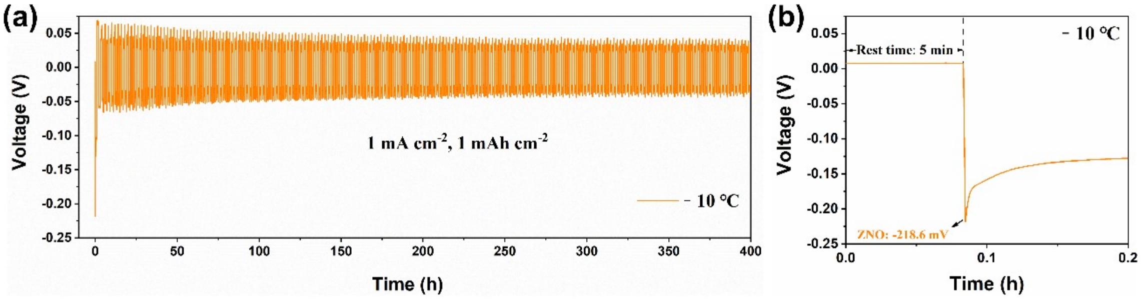

Fig. S1 Zn stripping/plating performance (a) and ZNO (b) of Zn anode cycled at -10 °C.

As expected (**Fig. S1**), the bare Zn anode at a lower temperature of -10 °C also exhibits an extended cycling life of 400 h without failure, but with the highest ZNO of -218.6 mV to initiate the Zn nucleation compared to that cycling at 0 °C (-152.8 mV), 20 °C (-121.5 mV), and 50 °C (-113.7 mV). This might be due to the sluggish Zn^{2+} transportation kinetics at low temperatures, which would intensify the Zn electrode polarization but help induce facile Zn-ion stripping/plating, contributing to the high stability and reversibility of Zn metal anodes.

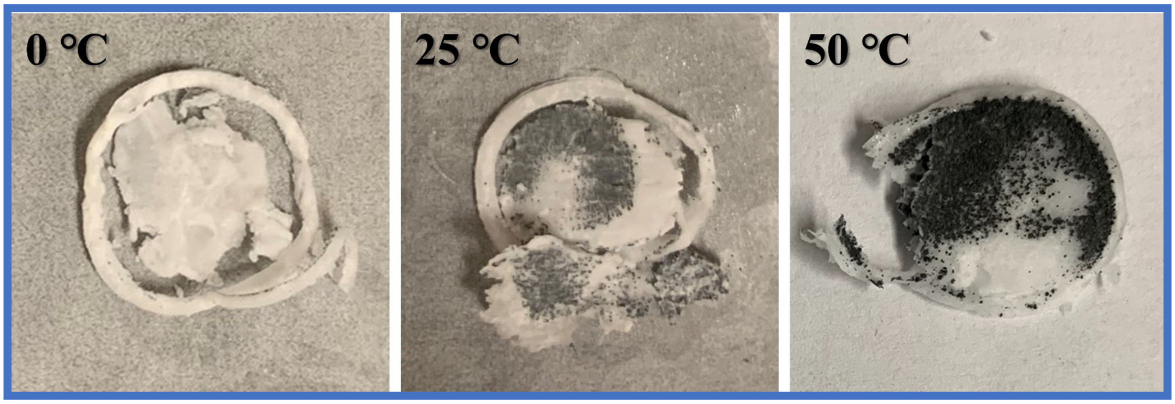

Fig. S2. SEM images of the glass-fiber separators recovered from the Zn|Zn cells at 0 °C, 20 °C, and 50 °C.

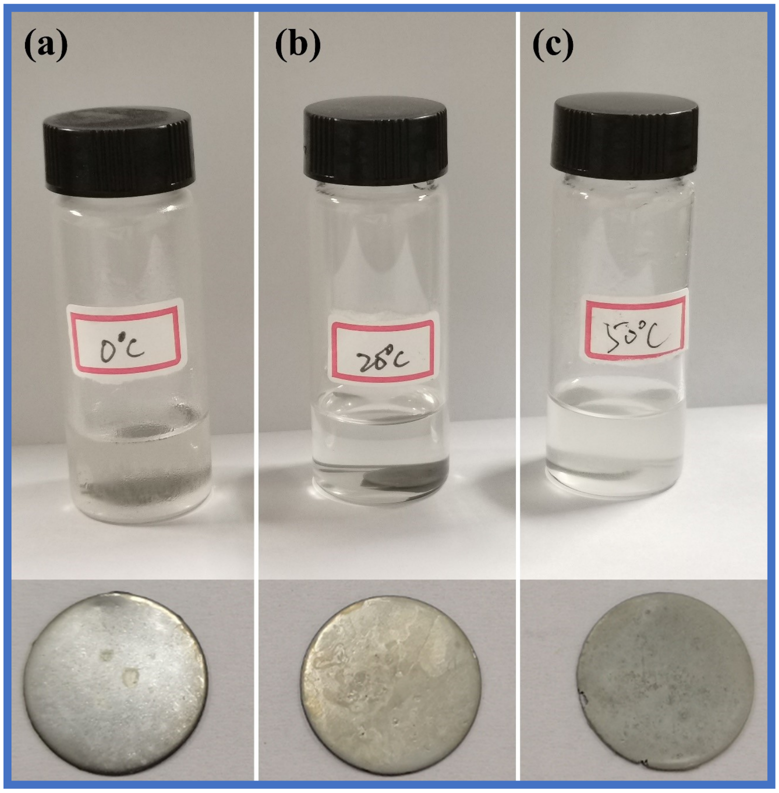

Fig. S3 Optical images of Zn foils stored at 0 ℃ (a), 20 ℃ (b) and 50 ℃ (c) in 3 M $Zn(CF_3SO_3)_2$ aqueous electrolyte for one week

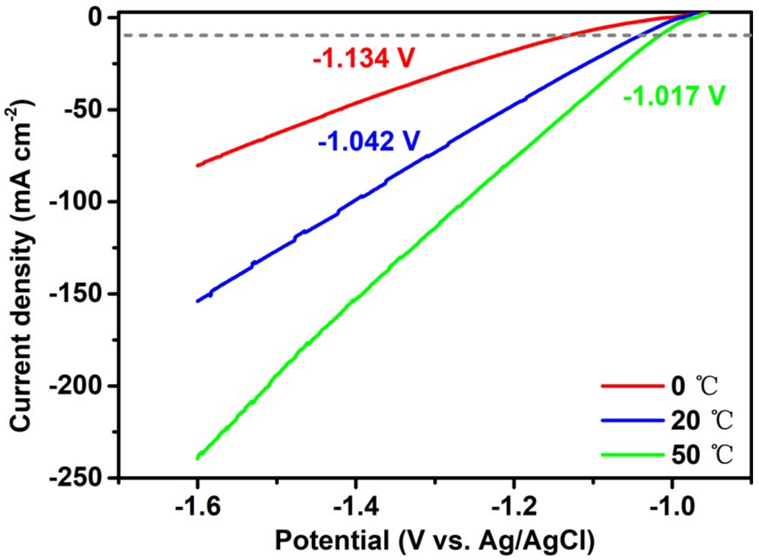

Fig. S4 HER curve of Zn anode measured at 0, 20, and 50 °C.

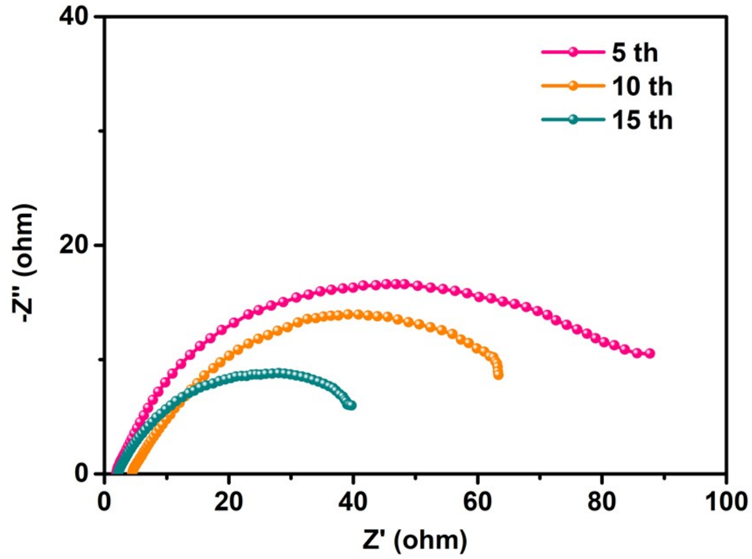

Fig. S5 EIS spectra of Zn symmetric cells cycled at 0 ℃.

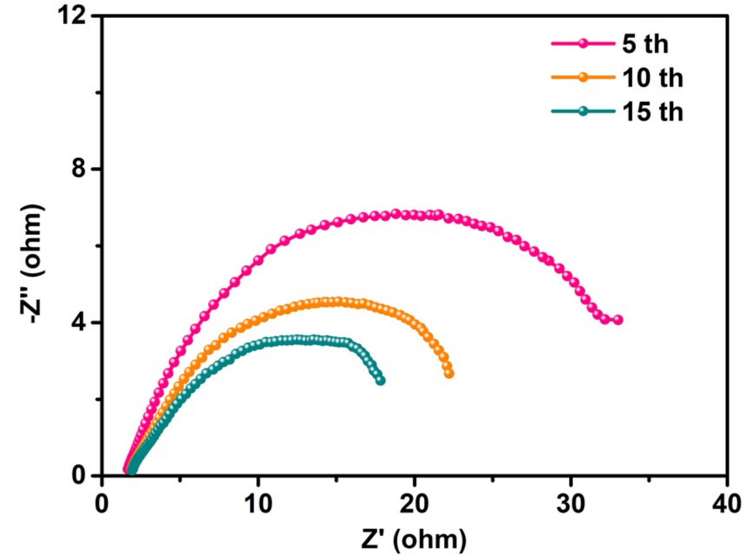

Fig. S6 EIS spectra of Zn symmetric cells cycled at 20 ℃.

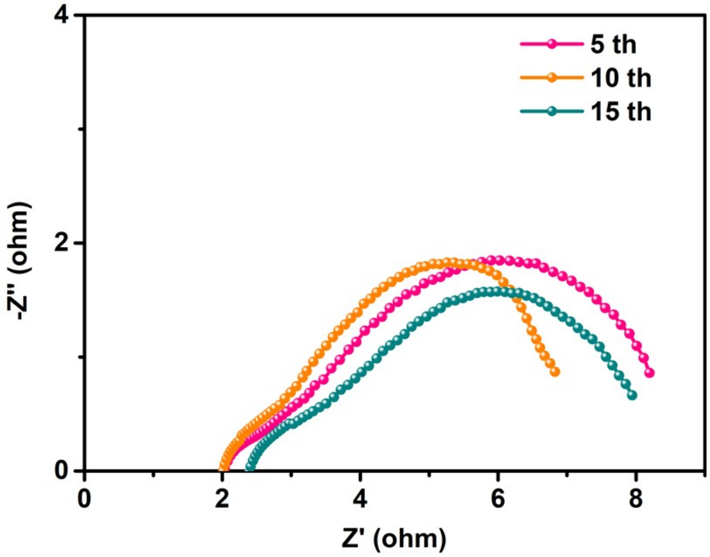

Fig. S7 EIS spectra of Zn symmetric cells cycled at 50 °C.

1. M. Zhou, S. Guo, G. Z. Fang, H. M. Sun, X. X. Cao, J. Zhou, A. Q. Pan and S. Q. Liang, *J. Energy Chem.*, 2021, **55**, 549.
2. Y. Yang, C. Liu, Z. Lv, H. Yang, Y. Zhang, M. Ye, L. Chen, J. Zhao and C. C. Li, *Adv. Mater.*, 2021, **33**, e2007388.
3. J. Hao, B. Li, X. Li, X. Zeng, S. Zhang, F. Yang, S. Liu, D. Li, C. Wu and Z. Guo, *Adv. Mater.*, 2020, **32**, e2003021.
4. Z. Li, W. Deng, C. Li, W. Wang, Z. Zhou, Y. Li, X. Yuan, J. Hu, M. Zhang, J. Zhu, W. Tang, X. Wang and R. Li, *J. Mater. Chem. A*, 2020, **8**, 17725.
5. L. T. Hieu, S. So, I. T. Kim and J. Hur, *Chem. Eng. J.*, 2021, **411**, 128584.
6. P. Chen, X. Yuan, Y. Xia, Y. Zhang, L. Fu, L. Liu, N. Yu, Q. Huang, B. Wang, X. Hu, Y. Wu and T. van Ree, *Adv. Sci.*, 2021, **8**, e2100309.
7. M. Li, Q. He, Z. L. Li, Q. Li, Y. X. Zhang, J. S. Meng, X. Liu, S. D. Li, B. K. Wu, L. N. Chen, Z. Liu, W. Luo, C. H. Han and L. Q. Mai, *Adv. Energy Mater.*, 2019, **9**, 1901469.
8. Q. Yang, Y. Guo, B. Yan, C. Wang, Z. Liu, Z. Huang, Y. Wang, Y. Li, H. Li, L. Song, J. Fan and C. Zhi, *Adv. Mater.*, 2020, **32**, e2001755.

9. A. Xia, X. Pu, Y. Tao, H. Liu and Y. Wang, *Appl. Surf. Sci.*, 2019, **481**, 852-859.